JOURNAL OF MATERIALS SCIENCE 31 (1996) 6215–6222

A process model for active brazing of ceramics

Part I *Growth of reaction layers*

T. TORVUND, Ø. GRONG
Norwegian University of Science and Technology, Department of Metallurgy, N-7034 Trondheim, Norway

O. M. AKSELSEN, J. H. ULVENSØEN
Sintef-Materials Technology, N-7034 Trondheim, Norway

In the present investigation process modelling techniques have been applied to describe reaction layer growth during active brazing of ceramics. As a starting point, the classical solution for parabolic growth of transformation products is considered. Specific computational features are then explicitly built into the model to allow for transient effects during heating and cooling as well as changes in the growth kinetics due to depletion of the active element during brazing. This approach gives considerable scope for optimization of both process and joint properties through adjustment of the filler metal composition and the temperature–time programme under which brazing takes place. The aptness of the process model is illustrated in an accompanying paper (Part II).

Nomenclature

A, $C_\gamma B_\delta$, $C_\varepsilon A_\eta$	reaction products in diffusion couple
$A_\alpha B_\beta$	ceramic component
C	reactive element in braze alloy
C_B	concentration of element B at a given position within the reaction layer, $C_\gamma B_\delta$ (mole m^{-3})
C_B^b	bulk concentration of element B in ceramic, $A_\alpha B_\beta$ (mole m^{-3})
$C_B^i(1)$, $C_B^i(2)$	concentration of element B in reaction layer at $C_\gamma B_\delta/A_\alpha B_\beta$ and braze metal/$C_\gamma B_\delta$ interface, respectively (mole m^{-3})
C_C	concentration of element C at a given position within the reaction layer, $C_\gamma B_\delta$ (mole m^{-3})
C_C^0	initial concentration of element C in braze metal (mole m^{-3})
C_C^b	bulk concentration of element C in braze metal (mole m^{-3})
$C_C^i(1)$, $C_C^i(2)$	concentration of element C in reaction layer at braze metal/$C_\gamma B_\delta$ and $C_\gamma B_\delta/A$ interface, respectively (mole m^{-3})
D_0, D_0^*	constants in expression for diffusion coefficient (m^2 s^{-1})
D_B	intrinsic diffusivity of B in $C_\gamma B_\delta$ (m^2 s^{-1})
D_C	intrinsic diffusivity of C in $C_\gamma B_\delta$ (m^2 s^{-1})
J_B	molar flux of element B (mole m^{-2} s^{-1})
J_C	molar flux of element C (mole m^{-2} s^{-1})
k_0	constant in expression for k_p (m^2 s^{-1})
k_0^*	rate constant referring to infinite diffusion couple analogue (m^2 s^{-1})
k_p	parabolic growth rate constant (m^2 s^{-1})
L	half width of braze metal zone (m)
m	proportionality constant (equal to the ratio between $C_C^i(1)$ and C_C^b)
Q_{app}	apparent activation energy for diffusion of C in $C_\gamma B_\delta$ (J mole^{-1})
Q_{app}^*	apparent activation energy for diffusion of B in $C_\gamma B_\delta$ (J mole^{-1})
R	universal gas constant (8.314 J mole^{-1} K^{-1})
t	time (s)
t_0	incubation time (s)
t_1, t_2	limits of integration (s)
t_i	isothermal hold time (s)
Δt_i	time increment used in the numerical integration procedure (s)
T	absolute temperature (K or °C)
T_c	chosen reference temperature (K or °C)
T_i	isothermal hold temperature (K or °C)
X	thickness of reaction layer (m)
X_c	contribution of the cooling leg of the brazing cycle to the total reaction layer thickness (m)
X_h	contribution of the heating leg of the brazing cycle to the total reaction layer thickness (m)
X_i	contribution of the isothermal hold period to the total reaction layer thickness (m)
X_{lim}	limiting thickness of reaction layer, $C_\gamma B_\delta$ (m)
ΔX_i	increase in reaction layer thickness due to a small time increment Δt_i (m)
y_1, y_2, y_3	molar partitioning factors
$\alpha, \beta, \gamma, \delta, \varepsilon, \eta$	molar stoichiometric factors
Ω	molar volume of reaction product, $C_\gamma B_\delta$ (m^3 mole^{-1})

0022–2461

1. Introduction

The brazing of ceramics is normally performed with the use of active filler metals in order to promote wetting and subsequent bonding of the materials [1]. The expression "active brazing" refers to a situation where strong oxide and nitride formers such as titanium or zirconium are added to the filler metal. Their role is mainly to facilitate the formation of a reaction layer at the boundary between the braze metal and the ceramic, which, in turn, can help to ensure intimate interfacial contact and hence a high bond strength [2–5].

There is considerable circumstantial evidence available in the scientific literature that the mechanical integrity of brazed ceramic–ceramic joints is strongly affected by the type and thickness of the reaction layer formed during brazing [4, 5]. For example, it has been shown that, in Al_2O_3–Al_2O_3 components joined with Ag–Cu–Ti filler metals, a reaction layer thickness of about 2 μm is required to achieve an optimum shear strength [6]. At larger layer thicknesses the bond strength tends to decrease, probably because the reaction product itself provides a preferred site for cracking, both in-plane and through-thickness relative to the layer. The bonding mechanism appears thus to be analogous to that documented for metal matrix composites, where the presence of a thin (crack-free) reaction layer adjacent to the reinforcement is often seen to improve the subsequent strength of the component. This improvement is due to the combined effect of a high frictional sliding resistance and an increased elastic modulus of the interface [7].

In practice, the extent of chemical reaction occurring between the braze metal and the parent ceramic material depends on the interplay between a number of variables which cannot readily be accounted for in a simple mathematical simulation of the process (e.g., thermodynamics and phase relations, element diffusivity, and the temperature–time programme) [8]. In the latter case the heating and cooling legs of the brazing cycle will also be of importance, since optimum joint properties suggest that the width of the reaction layer should be restricted to only a few micrometres. The inherent non-isothermal nature of the brazing process has previously been disregarded in the scientific literature, but the implications for reaction layer growth can be readily documented by means of process modelling techniques. By this we mean a simplified analytical treatment, based on the classical solution for parabolic growth of transformation products, using a personal computer. Although the present analysis does not offer a full physical record of the reaction mechanisms involved, it may provide the reader with valuable insights into the behaviour of ceramics during active brazing and can serve as a means to assemble information about the process. In addition, it may also shed new light upon reaction layer growth in general during thermal processing of composites, and fit some of the apparently conflicting results into a more consistent picture.

Application of the process model for the optimization of brazing conditions and joint properties for specific ceramic–metal combinations is described in an accompanying paper (Part II [9]).

2. The scope of this work

Whereas diffusion in binary systems can be subjected to an exact analytical treatment [10, 11], diffusion in multicomponent systems cannot be treated with the same degree of mathematical precision because of the complexity of the rate phenomena involved [8, 12, 13]. Additional problems result from the lack of adequate thermodynamic data, and the fact that some of the constituent elements may diffuse up their own concentration gradient as opposed to the binary case where the concentration and activity gradients usually have the same direction (an exception is a binary system with a solid miscibility gap) [8]. In order to proceed, it is therefore necessary to make a clear statement of the modelling objectives and the underlying assumptions on which the model is based. In the last resort, the justification relies on a good agreement between theory and experiments.

2.1. Model inputs

A generic ternary phase diagram provides a good starting point for assessment of phase relations during the brazing of ceramics with active filler metals. This, coupled with knowledge of the diffusion path, makes it possible to estimate the composition of the reaction layer, as shown schematically in Fig. 1(a and b). Unfortunately, data for diffusion coefficients in multicomponent systems are scarce and rather unreliable, which implies that the diffusion path, in practice, cannot be predicted from first principles [8]. Hence, detailed information about constituent phases and parabolic growth rate constants must be obtained from dedicated experiments. In practice, this means that the unknown kinetic constants are determined by fitting the integrals at fixed points to data for the reaction layer thickness. There are well accepted precedents for this in the scientific literature as an alternative to physical modelling [14].

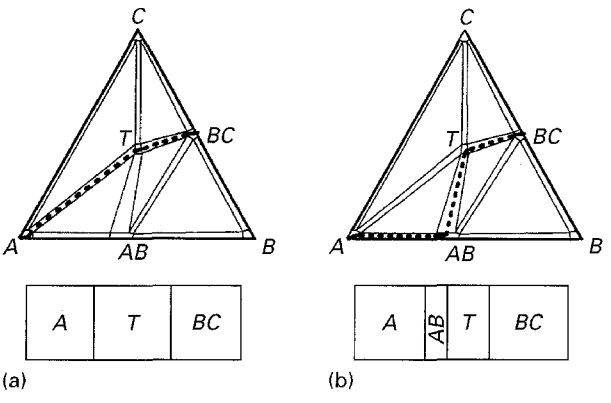

Figure 1 Ternary diffusion couple, *A–BC*, with different diffusion paths and reaction layers (schematic); (a) one layer (*T*), and (b) two layers (*T* + *AB*).

2.2. Model outputs

Since the problem of interest is reaction layer growth during active brazing, the constitutive evolution equation must be written in a differential form in order to incorporate the effect of the main process variables on the reaction kinetics. In particular, attempts will be made to illustrate the important difference between a finite and an infinite diffusion couple (finite in the sense that the supply of the reactive element is restricted), and document the individual contributions from the heating leg, the isothermal hold period, and the cooling leg of the brazing cycle on the total layer growth. This approach gives considerable scope for optimization of both process and joint properties through adjustment of the filler metal composition and the temperature–time programme under which brazing takes place.

3. Mathematical modelling

Diffusion in nonmetals such as ceramics, is very complex, and involves transport of both cations, anions and vacancies in a manner that enforces local equilibrium and charge neutrality within the crystal [15]. In the following, a simple physical framework for modelling reaction layer growth is presented, based on the assumption that the kinetics are controlled by transport of specific constituent elements through the product layers via a coupled cation or anion vacancy diffusion mechanism. This implies that there is no interaction between the transferring elements and the surroundings, and that the driving force for the reaction is provided by the concentration gradient rather than the activity (i.e., the chemical potential) gradient across the reaction zone. The conditions described above conform to bulk diffusion in a diluted ion matrix, and provide a means of modelling reaction layer growth during active brazing of ceramics.

3.1. Displacement reactions

In active brazing the occurrence of displacement reactions between the braze metal and the ceramic is an important consideration, and this has been exploited by several investigators in the past to model reaction layer growth in solid state diffusion couples [11, 16, 17]. Consider the following simple displacement reaction involving the reactive element C, the ceramic component $A_\alpha B_\beta$, and the reaction products $C_\gamma B_\delta$ and A with no mutual solubility between the phases:

$$y_1 A_\alpha B_\beta + C = y_2 C_\gamma B_\delta + y_1 \alpha A \qquad (1)$$

where α, β, γ and δ are the pertinent molar stoichiometric factors, and y_1 and y_2 are the molar partitioning fractions of $A_\alpha B_\beta$ and $C_\gamma B_\delta$, respectively.

Provided that the Gibbs free energy change per mole of the diffusate is negative, the reaction will proceed at a rate which is determined by transport of the reactants through the product layers. Fig. 2(a–c) shows schematic illustrations of the resulting product morphologies for the two extreme cases where the growth kinetics are controlled by diffusion of C-ions in $C_\gamma B_\delta$ and B-ions in A, respectively. In the former case the $A/C_\gamma B_\delta$ interface becomes essentially flat, as indicated in Fig. 2(b). This is because the flux of C-ions arriving at position I exceeds that at position II in Fig. 2(a), which means that possible interface perturbations tend to be unstable [8]. The situation is different when the reaction is controlled by diffusion of B-ions through the metal layer A. Under such conditions the growth kinetics will favour the formation of a wavy interface [8], leading to the aggregated morphology shown in Fig. 2(c).

In practice, full partioning of the phases, according to the scheme outlined in Fig. 2(a–c) refers to equilibrium conditions following prolonged high temperature annealing. In brazing, where transient effects are more predominant, it is often a reasonable approximation to assume that the displacement reaction is completely dominated by a single diffusion mechanism. When the rate controlling step is diffusion of C-ions in the product layer, the reaction will occur at the $C_\gamma B_\delta/A_\alpha B_\beta$ interface. Depending on the circumstances, the secondary reaction product A is either trapped in the primary phase or transported to the braze metal zone by diffusion (see Fig. 3(a)). Similarly, the assumption of highly mobile B-ions implies that the reaction takes place at the $C_\gamma B_\delta$/braze metal interface, as shown in Fig. 3(b). In both cases the secondary reaction product A may combine with the reactive element C to form an intermetallic compound $C_\varepsilon A_\eta$, according to the overall reaction:

$$y_1 A_\alpha B_\beta + C = y_2 C_\gamma B_\delta + y_3 C_\varepsilon A_\eta \qquad (2)$$

where y_3 is the corresponding molar partitioning fraction of the $C_\varepsilon A_\eta$ phase. Conservation of matter in Equation 2 requires, in turn, that y_1, y_2 and y_3 are related to α, β, γ, δ, ε and η as:

$$y_1 = \frac{1}{(\beta\gamma/\delta + \alpha\varepsilon/\eta)}, \quad y_2 = \frac{\beta}{\delta} y_1, \quad y_3 = \frac{\alpha}{\eta} y_1 \qquad (3)$$

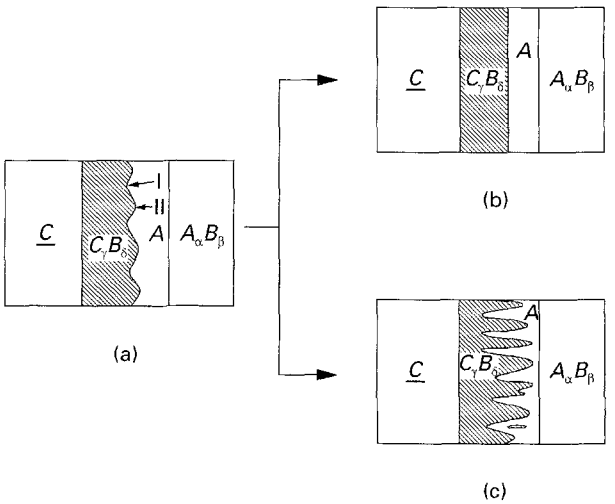

Figure 2 Schematic illustrations of some possible product morphologies according to reaction (1); (a) initial perturbed $C_\gamma B_\delta/A$ interface, (b) layered arrangement due to rapid diffusion of C-ions in $C_\gamma B_\delta$, (c) aggregated arrangement due to rapid diffusion of B-ions in metal layer A. The diagrams are based on the ideas of van Loo [8].

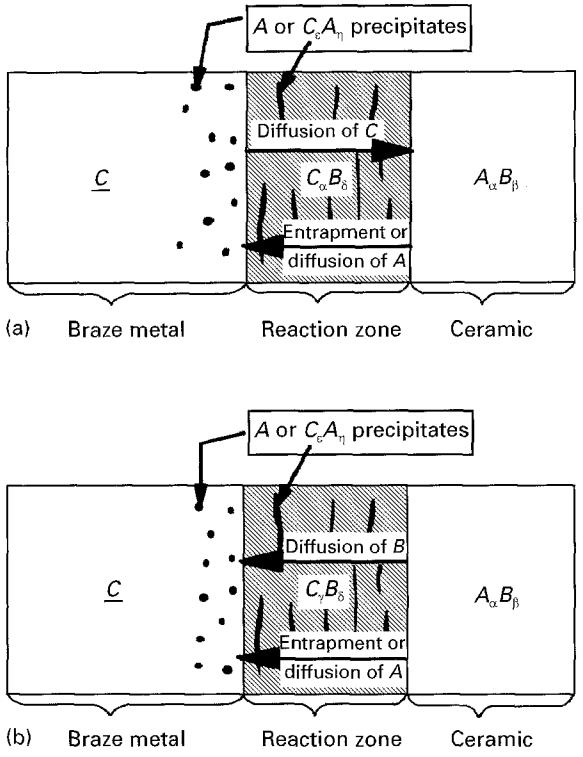

Figure 3 Simplified model systems for reaction layer growth during active brazing of ceramics; (a) highly mobile *C*-ions, (b) highly mobile *B*-ions.

In the following, the kinetics of reaction layer growth during active brazing of ceramics will be discussed in the light of these two diffusion mechanisms.

3.2. Finite diffusion couple analogue

Based on Fick's first law, it is possible to obtain a simple expression for the molar flux of $C(J_C)$ passing through the reaction zone per unit area and time for the diffusion couple considered in Fig. 4(a):

$$J_C = -D_C \frac{\partial C_C}{\partial X} \tag{4}$$

Here D_C is the intrinsic diffusivity of C in $C_\gamma B_\delta$, and C_C is the molar concentration of element C at a given position within the reaction layer (in mole m^{-3}).

It follows from Equation 2 that for each mole of C transported through the layer, y_2 moles of $C_\gamma B_\delta$ will form. Hence, the $C_\gamma B_\delta/A_\alpha B_\beta$ interface will advance relatively to the $C_\gamma B_\delta$/filler metal interface by a rate defined as:

$$\frac{dX}{dt} = -y_2 \Omega D_C \frac{\partial C_C}{\partial X} \tag{5}$$

where Ω is the molar volume of the $C_\gamma B_\delta$ phase (in m^3 mole^{-1}).

Equation 5 may be further simplified if the concentration gradient within the $C_\gamma B_\delta$ phase is approximated by that of a straight line extending from C_C^i (1) to C_C^i (2) (see Fig. 4(a)). Taking Q_{app} equal to the

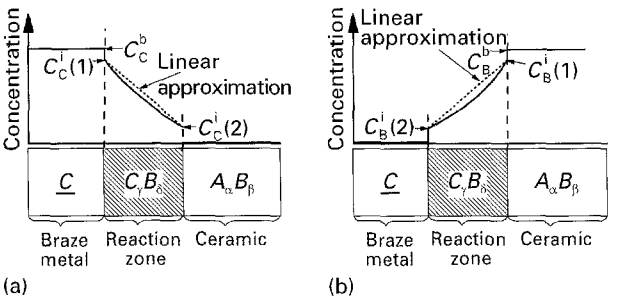

Figure 4 Sketch of diffusion couples and resulting concentration profiles across the reaction zone for different operating conditions; (a) finite diffusion couple analogue, (b) infinite diffusion couple analogue.

apparent activation energy for diffusion of C in $C_\gamma B_\delta$ and C_C^i (1) $\gg C_C^i$ (2), we obtain:

$$\frac{dX}{dt} \approx y_2 \Omega D_0 \exp\left(-\frac{Q_{app}}{RT}\right)\frac{C_C^i(1)}{X} \tag{6}$$

Provided that Equation 6 contains separable variables of X and T, it may be integrated as follows:

$$X^2 = \int_{t_1}^{t_2} 2y_2 \Omega D_0 C_C^i(1) \exp\left(-\frac{Q_{app}}{RT}\right) dt \tag{7}$$

where the limits t_1 and t_2 refer to the total time spent in the thermal cycle from the chosen reference temperature T_C to the isothermal hold temperature T_i and down again to T_C.

Based on chemical thermodynamics, it can be argued that the interface concentration $C_C^i(1)$ will differ from the bulk concentration C_C^b only by a proportionality constant, m. By introducing the parabolic growth rate constant $k_p = k_0 \exp(-Q_{app}/RT)$ for the reaction, we see that k_0 is of the form:

$$k_0(m^2 s^{-1}) = 2y_2 \Omega D_0 C_C^i(1) = 2y_2 \Omega D_0 m C_C^b \tag{8}$$

from which

$$X^2 = \int_{t_1}^{t_2} k_0 \exp\left(-\frac{Q_{app}}{RT}\right) dt \tag{9}$$

Since k_0 depends on C_C^b, the rate constant will gradually decrease as the reactive element C is consumed during the brazing cycle. This means that Equation 6 is not separable under the prevailing conditions. Based on a simple mass balance, it is possible to define an upper limit for the thickness of the reaction layer, conforming to the situation where all C is tied up as $C_\gamma B_\delta$ (and $C_\varepsilon A_\eta$). Let L denote the half width of the braze metal zone, and C_C^0 the initial content of C in the alloy. Then the limiting thickness of the $C_\gamma B_\delta$ layer, X_{lim}, is given as:

$$X_{lim} = y_2 L \Omega C_C^0 \tag{10}$$

Similarly, for a layer thickness $X < X_{lim}$, we may write:

$$X = y_2 L \Omega (C_C^0 - C_C^b) \tag{11}$$

where C_C^b is the instantaneous concentration of element C. From Equations 8, 10 and 11 we see that k_0 scales with X and X_{lim} as:

$$k_0 = k_0^* \frac{X_{lim} - X}{X_{lim}} \quad (12)$$

where k_0^* is the corresponding rate constant for the infinite diffusion couple analogue (assuming abundant supply of reactive element, i.e., $C_C^b = C_C^0$).

Because k_0 depends on X, the solution of the differential evolution equation requires stepwise integration in temperature–time space over the predetermined thermal cycle, using an appropriate numerical integration procedure. The following algorithms are defined for this purpose, based on Equations 9 and 12:

$$\sum_{i=1}^{n} (\Delta X_i^2) = k_0^* \sum_{i=1}^{n} \exp\left(-\frac{Q_{app}}{RT_i}\right) \Delta t_i \quad (13)$$

and

$$X = \left[\sum_{i=1}^{n} (\Delta X_i^2) \frac{X_{lim} - \left(\sum_{i=1}^{n} (\Delta X_i^2)\right)^{1/2}}{X_{lim}} \right]^{1/2} \quad (14)$$

Equations 13 and 14 provide a basis for predicting the evolution of the reaction layer during active brazing of ceramics for a wide range of operational conditions, provided that the process is controlled by diffusion of the reactive component C within the $C_\gamma B_\delta$ phase.

3.3. Infinite diffusion couple analogue

In this case the situation is slightly different. Referring to Fig. 4(b), the assumption of an infinite diffusion couple (i.e., highly mobile B-ions) implies that the molar flux J_B passing through the reaction zone per unit area and time is given as:

$$J_B = -D_B \frac{\partial C_B}{\partial X} \quad (15)$$

where D_B is the intrinsic diffusivity of B in $C_\gamma B_\delta$, and C_B is the molar concentration of element B in an arbitrary position within the reaction layer. Under such conditions, the braze metal/$C_\gamma B_\delta$ interface will advance at a rate defined by:

$$\frac{dX}{dt} = y_2 \Omega D_B \frac{\partial C_B}{\partial X} \quad (16)$$

If we, as in the previous case, assume a linear concentration gradient across the reaction zone, take Q_{app}^* equal to the apparent activation energy for diffusion of B in $C_\gamma B_\delta$ and $C_B^i(1) \gg C_B^i(2)$, Equation (16) reduces to a first order separable differential equation:

$$\frac{dX}{dt} \approx y_2 \Omega D_0^* \exp\left(-\frac{Q_{app}^*}{RT}\right) \frac{C_B^i(1)}{X} \quad (17)$$

which after integration and substitution yields:

$$X^2 = \int_{t_1}^{t_2} 2y_2 \Omega D_0^* C_B^i(1) \exp\left(-\frac{Q_{app}^*}{RT}\right) dt$$

$$= k_0^* \int_{t_1}^{t_2} \exp\left(-\frac{Q_{app}^*}{RT}\right) dt \quad (18)$$

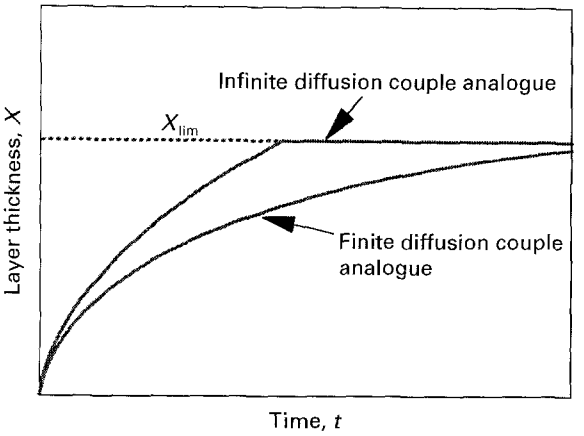

Figure 5 The difference between an infinite and a finite diffusion couple analogue according to Equation 18 and Equations 13 and 14, respectively (schematic).

Since the rate constant k_0^* does not depend on C_C^b, the right-hand side of Equation (18) represents the "kinetic" strength of the brazing cycle with respect to reaction layer growth. This integral can readily be evaluated by means of numerical methods when the thermal programme is known. Equation (18) differs from Equations 13 and 14 in that the reaction layer thickness in the former relation is not contingent upon the supply of reactive element C as long as $X < X_{lim}$. In practice, this means that the growth process suddenly stops when $X = X_{lim}$, while the assumption of a finite diffusion couple (i.e., highly mobile C-ions) implies that X_{lim} is approached in an asymptotic manner, as illustrated schematically in Fig. 5.

4. Comparison with experiments

In the following, the models will be tested against experimental data obtained from various sources. Referring to Fig. 6 the method adopted here is based on the idea of integrating the differential evolution equations over the brazing cycle where the unknown kinetic constants (here k_0^*, Q_{app} or Q_{app}^*) are determined by fitting the integrals at certain fixed points to data for the reaction layer thickness. These represent a wide spectrum of ceramic–metal combinations and provide a means of checking the validity of the models under different brazing conditions.

4.1. Brazing of Al_2O_3 with Cu–Ti and Cu–Zr filler metals

The Al_2O_3/Cu–Ti system and the corresponding Al_2O_3/Cu–Zr system have been previously examined by Bang *et al.* [18]. Here bonding is achieved by reduction of Al_2O_3 according to the overall displacement reactions:

$$3Ti + Al_2O_3 = 3TiO + 2Al \quad (19)$$

and

$$3Zr + 2Al_2O_3 = 3ZrO_2 + 4Al \quad (20)$$

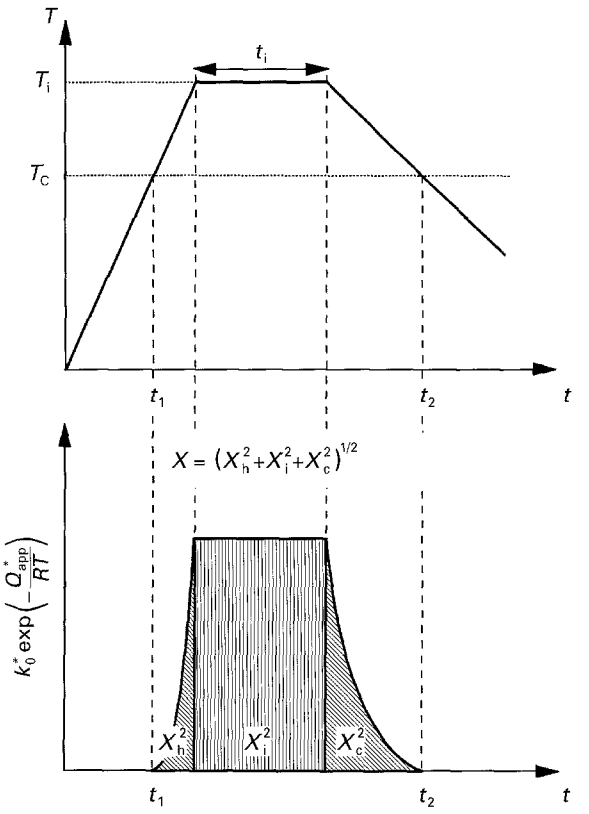

Figure 6 Schematic diagrams defining the kinetic strength of a brazing cycle with respect to reaction layer growth. The parameters X_h, X_i and X_c refer to the individual contributions of the heating leg, the isothermal hold period and the cooling leg of the brazing cycle to the total layer thickness, respectively.

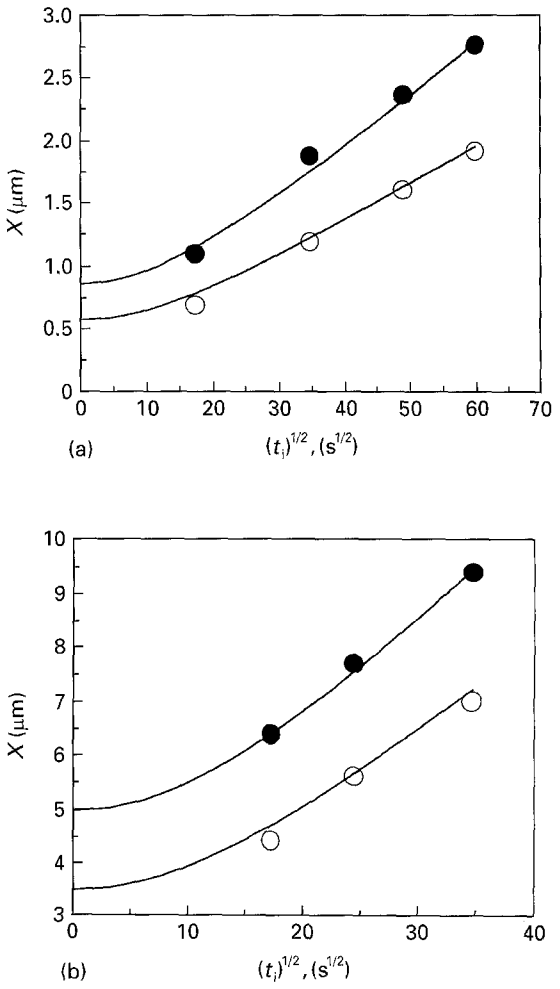

Figure 7 Comparison between measured and predicted reaction layer thicknesses during brazing of Al_2O_3 with Cu–Ti and Cu–Zr filler metals; (a) Al_2O_3/Cu–Ti system at (●) 1373 and (○) 1323 K, (b) Al_2O_3/Cu–Zr system at (●) 1373 K and (○) 1323 K. Input data from Bang *et al.* [18] and Table I.

In both cases the growth process is believed to be controlled by diffusion of oxygen ions through the reaction layer [18], which suggests that the systems can be treated as infinite diffusion couple analogues. Fig. 7(a and b) show a comparison between predictions and measurements, using the input data listed in Table I. A closer inspection of the graphs reveals that the overall agreement is satisfactory in the sense that the data points are well represented by the model predictions. Moreover, it is interesting to note that the relationship between the layer thickness, X, and the square root of the isothermal hold time, t_i, appears to be nonlinear rather than linear during the early stages of the growth process. This is due to the contributions of the heating and cooling leg of the brazing cycle to the total layer thickness (X_h and X_c, respectively), which according to Fig. 6 amounts to:

$$X = (X_h^2 + X_c^2 + X_i^2)^{1/2} = (X_h^2 + X_c^2 + k_p t_i)^{1/2} \quad (21)$$

It follows from Equation (21) that a linear relationship between X and $t_i^{1/2}$ is only to be expected when the product $k_p t_i \gg X_c^2 + X_h^2$. This important point has previously been overlooked in the scientific literature.

4.2. Brazing of Si_3N_4 with different Cu-based filler metals

Bonding of Si_3N_4 to refractory metals such as W, Mo and Ta with Cu-based braze alloys has been investigated by Nakao *et al.* [19]. During brazing a wide range of reaction products can form at the ceramic/braze alloy interface, depending on the type of active element present in the filler metal (e.g., Nb, Ti or Zr).

TABLE I Input data used in modelling of reaction layer growth for the Al_2O_3/Cu–20 wt % Ti and the Al_2O_3/Cu–5 wt% Zr system, respectively

System	Heating rate ($°C s^{-1}$)	Cooling rate ($°C s^{-1}$)	k_0^* ($\mu m^2 s^{-1}$)	Q_{app}^* ($kJ mole^{-1}$)	X_{lim} (μm)	T_c (°C)
Al_2O_3/Cu–Ti	1.2	0.2	1.6×10^5	208	33	915
Al_2O_3/Cu–Zr	1.2	0.2	0.29×10^5	156	15	1000

4.2.1. Cu–Nb filler metals

In this case the consumption of the active component can be described by the following displacement reaction [19]:

$$Si_3N_4 + 13Nb = 4NbN + 3Nb_3Si \qquad (22)$$

Since niobium combines with both silicon and nitrogen, the braze metal becomes rapidly depleted with respect to the reactive element. In practice, this is seen as a deviation from the parabolic growth law at long holding times [19], which suggests that the system can be treated as a finite diffusion couple analogue. Fig. 8(a) shows a comparison between measured and predicted reaction layer thickness, using input data from Table II. It is evident from these plots that the observed stagnation in the reaction layer growth is adequately accounted for in the model predictions. At the highest brazing temperature the limiting layer thickness of about 4.2 μm is approached after a holding time of about 900 s, while at lower temperatures longer holding times are needed to compensate for the associated reduction in element diffusivity. Although the present analysis does not offer a full physical record of the reaction mechanisms involved, it captures the essential features of the diffusion process by relating reaction layer growth to the content of the active element in the braze metal.

4.2.2. Cu–Ti filler metals

The Si_3N_4/Cu–Ti system provides another case of application of the process model. Under the prevailing conditions, titanium reacts with both nitrogen and silicon to form TiN and Ti_5Si_3, according to the overall displacement reaction [19]:

$$Si_3N_4 + 9Ti = 4TiN + Ti_5Si_3 \qquad (23)$$

Because of the abundant supply of titanium, the system can be treated as an infinite diffusion couple analogue where the lack of layer growth during the early stages of the process is accounted for by introducing an empirical incubation time t_0 in the evolution equation. The results from the model predictions are shown in Fig. 8(b), using input data from Table II. As seen from the figure, the use of an incubation time improves the confidence in the model predictions, although t_0, in the present case, has no direct physical meaning in the sense that it can be correlated to a specific diffusion blocking mechanism.

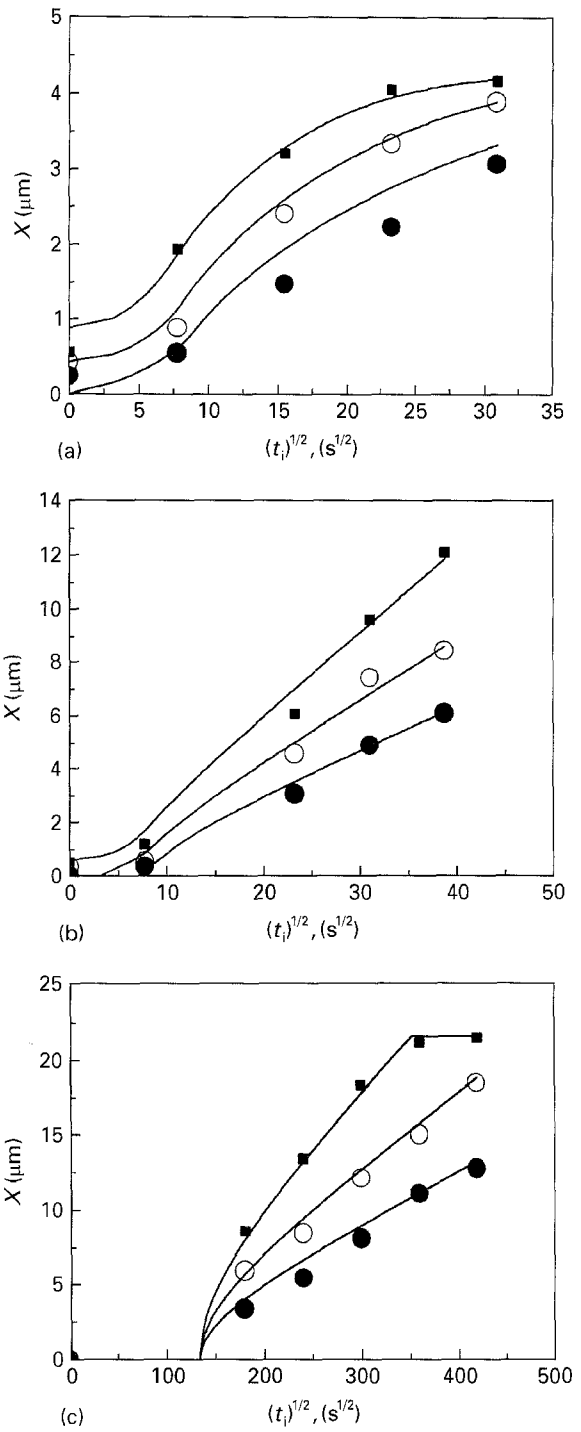

Figure 8 Comparison between measured and predicted reaction layer thicknesses during brazing of Si_3N_4 with Cu-based filler metals: (a) Si_3N_4/Cu–Nb system at (●) 1523 K, (○) 1548 K and (■) 1573 K; (b) Si_3N_4/Cu–Ti system at (●) 1348 K, (○) 1373 K and (■) 1398 K and (c) Si_3N_4/Cu–Zr system at (●) 1398 K, (○) 1423 K and (■) 1448 K. Input data from Nakao *et al.* [19] and Table II.

TABLE II Input data used in modelling of reaction layer growth for the Si_3N_4/Cu–1 wt % Nb, the Si_3N_4/Cu–5 wt % Ti and the Si_3N_4/Cu–10 wt % Zr system, respectively

System	Heating rate ($°C s^{-1}$)[a]	Cooling rate ($°C s^{-1}$)[a]	k_0^* ($\mu m^2 s^{-1}$)	t_0 (s)	Q_{app}^* ($kJ mole^{-1}$)	X_{lim} (μm)	T_c (°C)
Si_3N_4/Cu–Nb	1.5	1	7.2×10^{16}	140	536	4.2	1167
Si_3N_4/Cu–Ti	1.5	1	1.3×10^{14}	130	405	24	1030
Si_3N_4/Cu–Zr	1.5	1	2.2×10^{14}	18000	463	22	1000

[a]Estimated.

4.2.3. Cu–Zr filler metals

As a last example, we shall consider the Si_3N_4/Cu–Zr system, which may be treated as an infinite diffusion couple analogue with a sharp cut-off in the growth kinetics at $X = X_{lim}$. In this case the overall displacement reaction can be written as [19]:

$$Si_3N_4 + 9Zr = 4ZrN + Zr_5Si_3 \quad (24)$$

Once again, the lack of growth during the initial stages of the diffusion process is accounted for by the use of an empirical incubation time t_0 in the model predictions. It follows from Fig. 8(c) that the combination of parameters listed in Table II provides an adequate description of the experimental data both at high and low brazing temperatures. In particular, the abrupt change in the growth kinetics at $X = X_{lim}$ is obvious from these data.

5. Conclusions

In the present investigation, a process model has been developed which describes reaction layer growth during active brazing of ceramics. By solving the differential evolution equation for fixed starting conditions, the layer thickness can be calculated as a function of time and temperature when the following input data are available:

(i) Information about phase relations in the form of a stoichiometrically balanced displacement reaction.

(ii) Knowledge of the overall (rate controlling) diffusion mechanism and the temperature dependence of the parabolic growth rate constant for the infinite diffusion couple analogue.

(iii) Information about the initial content (mass) of reactive element in the braze metal.

(iv) Knowledge of the temperature–time pattern during brazing (including the transient heating and cooling period).

It is shown that extensive reaction layer growth may occur during the transient heating and cooling period. Moreover, depletion of the active element in the braze metal can give rise to a change in the growth kinetics, which is either abrupt or continuous, depending on the diffusion mechanism. Both factors contribute to a deviation from the parabolic growth law.

Acknowledgements

The authors acknowledge the financial support from Norsk Hydro (Porsgrunn, Norway), Elkem (Kristiansand, Norway) and the Research Council of Norway (Oslo, Norway). In addition, thanks are due to Øyvind Frigaard (Department of Metallurgy, Norwegian University of Science and Technology) for preparing the initial Turbo Pascal software package used to display the growth kinetics.

References

1. M. M. SCHWARTZ, "Ceramic Joining" (ASM International, Materials Park, OH, 1990).
2. M. BACKHAUS-RICOULT, in Proceedings of the International Workshop on Metal-Ceramic Interfaces, Santa Barbara, January 1989, edited by M. Rühle (Pergamon Press, Oxford, 1990) p. 79.
3. F. S. OKUCHI, *ibid.* p. 93.
4. K. SUGANUMA, *ISIJ International* **30** (1990) 1046.
5. O. M. AKSELSEN, *J. Mater. Sci.* **27** (1992) 1989.
6. H. HONGOI, J. ZHIHAO and W. XIAOTIAN, *ibid.* **29** (1994) 5041.
7. T. W. CLYNE and P. J. WITHERS, "An Introduction to Metal Matrix Composites" (Cambridge University Press, Cambridge, 1993).
8. F. J. J. VAN LOO, *Prog. Solid St. Chem.* **20** (1990) 47.
9. T. TORVUND, Ø. GRONG, O. M. AKSELSEN and J. H. ULVENSØEN, *J. Mater. Sci.* (in press).
10. C. WAGNER, *Acta Metall.* **17** (1969) 99.
11. D. S. WILLIAMS, R. A. RAPP and J. P. HIRTH, *Metall. Trans. A* **12A** (1981) 639.
12. J. S. KIRKALDY and L. C. BROWN, *Can. Metall. Quaterly* **2** (1963) 89.
13. L. S. K. HEIKINHEIMO, G. H. M. GUBBELS, G. de WITH and F. J. J. VAN LOO, in Proceedings of the 3rd International Conference on Brazing, High Temperature Brazing and Diffusion Welding, Aachen, November 1992, edited by E. Lugscheider (DVS, Düsseldorf, 1992) p. 87.
14. M. F. ASHBY, *Mater. Sci. Techn.* **8** (1992) 102.
15. P. SHEWMON, "Diffusion in Solids" 2nd Edn (TMS, Warrendale, PA 1989).
16. G. J. YUREK, R. A. RAPP and J. P. HIRTH, *Metall. Trans.* **4** (1973) 1293.
17. R. A. RAPP, A. EZIS and G. J. YUREK, *ibid.* 1283.
18. K. S. BANG, S. LIU and D. L. OLSON, in Proceedings of the 3rd International Conference on Trends in Welding Research, Gatlinburg, TN June 1992, edited by S. A. David and J. M. Vitek (ASM International, Materials Park, OH, 1992) p. 1129.
19. Y. NAKAO, K. NISHIMOTO and K. SAIDA, *Trans. Jpn. Weld. Soc.* **20** (1989) 66.

Received 18 August 1995
and accepted 17 July 1996